The Plant Cell, Vol. 17, 3337–3349, December 2005, www.plantcell.org © 2005 American Society of Plant Biologists

The *Arabidopsis thaliana* SOMATIC EMBRYOGENESIS RECEPTOR-LIKE KINASES1 and 2 Control Male Sporogenesis

Catherine Albrecht,[a] Eugenia Russinova,[a] Valerie Hecht,[b] Erik Baaijens,[a] and Sacco de Vries[a,1]

[a] Laboratory of Biochemistry, Department of Agrotechnology and Food Sciences, Wageningen University and Research Centre, 6703 HA Wageningen, The Netherlands

[b] School of Plant Science, University of Tasmania, Hobart, Tasmania 7001, Australia

The *Arabidopsis thaliana* SOMATIC EMBRYOGENESIS RECEPTOR-LIKE KINASE (SERK) family of plasma membrane receptors consists of five closely related members. The *SERK1* and *SERK2* genes show a complex expression pattern throughout development. Both are expressed in anther primordia up to the second parietal division. After this point, expression ceases in the sporocytes and is continued in the tapetum and middle layer precursors. Single knockout mutants of *SERK1* and *SERK2* show no obvious phenotypes. Double mutants of *SERK1* and *SERK2* are completely male sterile due to a failure in tapetum specification. Fertility can be restored by a single copy of either gene. The SERK1 and SERK2 proteins can form homodimers or heterodimers in vivo, suggesting they are interchangeable in the SERK1/SERK2 signaling complex.

INTRODUCTION

In plants, embryogenesis can be recapitulated starting from single somatic cells in culture (Reinert, 1959). This remarkable observation implies that plant cells are able to achieve totipotency long after completion of embryogenesis. Several genes have been described that alter the totipotency status of somatic cells, either upon mutation or after ectopic expression (reviewed in Mordhorst et al., 1997, 2005). The natural occurrence of parthenogenesis and apomixis and the ease by which embryogenesis can be initiated from microspores suggest that female and male gametophytic cells already contain the property to develop embryos prior to the occurrence of fertilization (Bicknell and Koltunow, 2004).

The *Daucus carota Somatic Embryogenesis Receptor-like Kinase* (Dc*SERK*) gene was found to be a marker for single embryogenic cells in culture (Schmidt et al., 1997). The predicted protein structure of the SERK proteins start at the N terminus with a signal peptide followed by a Leu zipper domain, five Leu-rich repeats (LRRs), a Pro-rich domain called the Ser-Pro-Pro motif, a single transmembrane domain, the 11 conserved subdomains of a Ser-Thr kinase, and a C-terminal Leu-rich domain (Hanks et al., 1988). The hallmark of the SERK proteins is the presence of the extracellular Ser-Pro-Pro motif in combination with precisely five LRRs.

According to the most recent annotation, the *Arabidopsis thaliana* (*SERK*) family of receptor kinases now consists of five closely related members (Hecht et al., 2001). They are annotated as *SERK1* to *SERK5* and all belong to subclass LRR II of the *Arabidopsis* receptor-like kinase (RLK) family (Shiu and Bleecker, 2001). The genomic organization of these genes is highly conserved (i.e., the intron–exon boundaries are in the same position in all five genes).

Overexpression of the *Arabidopsis* ortholog *SERK1*, closest to carrot Dc*SERK* in predicted protein sequence, resulted in enhanced formation of embryogenic cells in response to the growth regulator 2,4-D (Hecht et al., 2001). This supports the notion that SERK1-mediated signaling is involved in embryogenic cell formation. In planta, the SERK1 protein is located in the plasma membrane of both the male and female gametophytes as well as in surrounding sporophytic primordial cell layers. Later, the protein is found in all cells of the embryo and in seedlings predominantly in the vascular tissue of roots, shoots, and leaves. Lower levels of the protein are seen in epidermal cells, while formation of lateral roots appears to be accompanied with a higher level of SERK1 protein (Hecht et al., 2001; Kwaaitaal et al., 2005). Apparently, the signaling mediated by SERK1 is required in cells that retain or regain their embryogenic potential but is also required in cells that participate in organogenesis.

The *SERK2* gene is most closely related to *SERK1*, with an overall amino acid identity of 90%. Phylogenic analysis suggests that *SERK1* and *SERK2* have evolved by recent duplication and are closest homologues (Hecht et al., 2001).

The *SERK3* gene is identical to the recently described *BRI1-Associated Receptor Kinase1* (*BAK1*) gene, of which a knockout mutation results in a semidwarf phenotype, reminescent of weak alleles of the *brassinosteroid-insensitive1* (*BRI1*) receptor (Li et al., 2002; Nam and Li, 2002). SERK3 may be involved in relocalizing the BRI1 receptor via accelerated endocytosis (Russinova et al., 2004). BRI1 binds brassinosteroids directly, and this binding was not affected in a *bak1* background (Kinoshita et al., 2005), suggesting that BAK1 is a non-ligand-binding coreceptor of BRI1. In general, *bri1* mutants exhibit a much more severe phenotype than *bak1* (*serk3*) alleles, suggesting that BRI1

[1] To whom correspondence should be addressed. E-mail sacco.devries@wur.nl; fax 31-317-484801.

The author responsible for distribution of materials integral to the findings presented in this article in accordance with the policy described in the Instructions for Authors (www.plantcell.org) is: Sacco de Vries (sacco.devries@wur.nl).

Article, publication date, and citation information can be found at www.plantcell.org/cgi/doi/10.1105/tpc.105.036814.

is able to carry out the entire brassinolide signaling in the absence of BAK1 or that the BAK1 function is taken over by a close homologue. An alternative explanation would be that SERK3 controls only a subset of the BRI1-mediated effects resulting in only part of the complete brassinosteroid phenotypic defect. Candidates for genes carrying out other elements of the highly complex brassinosteroid defect would be other members of the *BRI* family (Caño-Delgado et al., 2004) and perhaps other members of the *SERK* family.

For the last members of the family, *SERK4* and *SERK5*, no additional evidence is currently available other then being predicted to be the closest paralogs of *SERK3* (*BAK1*).

In this work, we show that *SERK1* and *SERK2* genes are expressed in the same cells throughout development. SERK1 and SERK2 proteins can form either homodimers or heterodimers in vivo. We also present genetic evidence that SERK1 and SERK2 are functionally redundant and together control the formation of functional microspores.

RESULTS

Characterization of *SERK1* and *SERK2* Null Mutant Alleles

The *serk1-1* T-DNA–tagged allele was identified in the SIGnAL TDNA-Express collection as nr 044330. *serk1-1* has an insertion at nucleotide 3109 starting from the translation initiation codon. This corresponds to exon 11, encoding the last kinase subdomain XI and the C-terminal region of the protein (Hanks et al., 1988). The insertion leads to a truncated protein lacking the last 103 amino acids. DNA gel blot mapping confirms that *serk1-1* carries a T-DNA insertion in the expected genomic DNA fragments. No additional T-DNA insertions are detected in this line. *serk1-1* was backcrossed to Columbia wild type, and F1 and F2 progenies were analyzed for segregation of the kanamycin-resistant phenotype and the T-DNA insertion in *SERK1*. The F2 progeny segregated 3:1 (190 kanamycin-resistant plants:45 kanamycin-sensitive plants). Of 129 plants, PCR analysis showed that 30 were homozygous wild-type, 70 were heterozygotes, and 29 were homozygous T-DNA–tagged alleles. As such, the segregation ratio of the F2 progeny was approximately 1:2:1 (wild type:heterozygous:mutant), indicating a Mendelian segration for a single locus *serk1-1.* These data together with the DNA gel blot mapping are consistent with the fact that this T-DNA insertion line is a single insertion line in the *SERK1* gene.

The second allele, *serk1-2* (nr 053021), was characterized as described for *serk1-1* and has an insertion in exon 11, 87 bp downstream of the *serk1-1* insertion site leading to a truncated protein lacking the last 74 amino acids. The locations of the *serk1-1* and *serk1-2* T-DNA insertions are presented in Figure 1A.

The *serk2-2* T-DNA–tagged allele was identified in the Syngenta Arabidopsis Insertion Library (SAIL) lines (nr 119-G03). *serk2-2* has an insertion at nucleotide 1655 from the translation

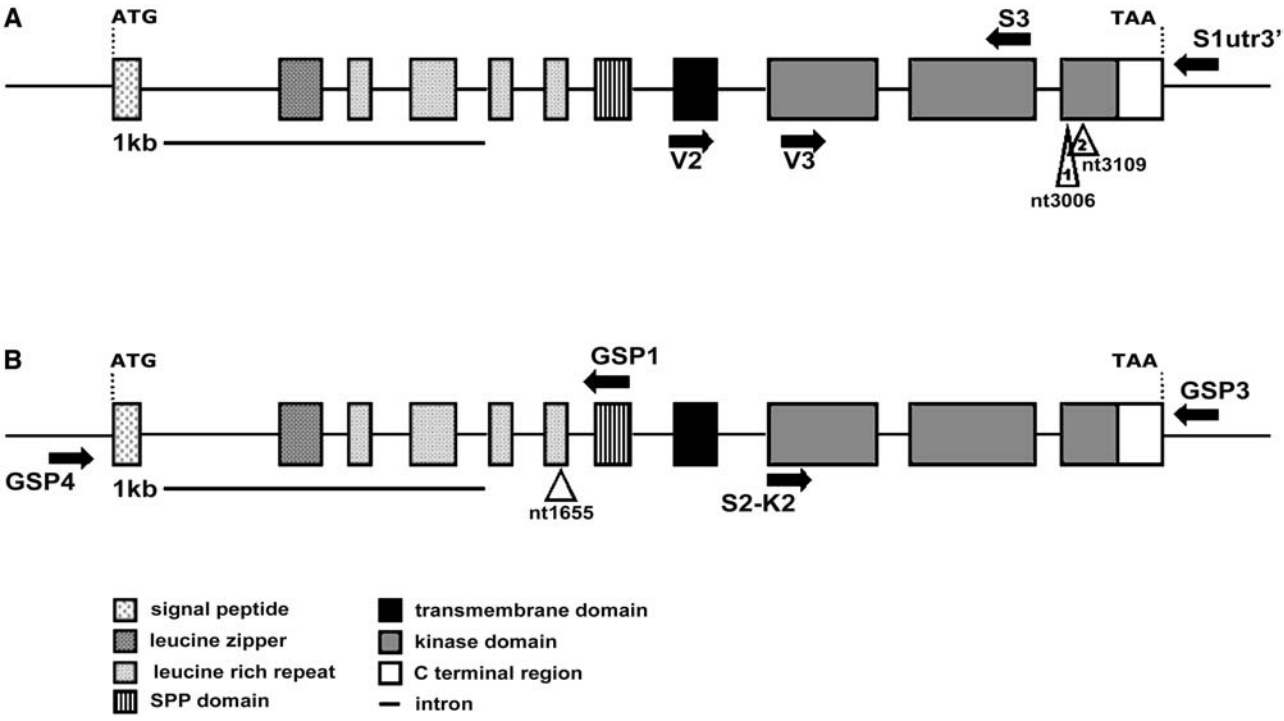

Figure 1. Characterization of *SERK1* and *SERK2* Loci.

(A) Characterization of the *SERK1* locus. Arrowheads 1 and 2 indicate the positions of the T-DNA insertions in *serk1-1* and *serk1-2* mutant alleles, respectively. The position of the primers used for RT-PCR and genotyping analysis is indicated. Bar = 1 kb.

(B) Characterization of the *SERK2* locus. The arrowhead indicates the position of the T-DNA insertion in the *serk2-2* mutant allele. The position of the primers used for RT-PCR and genotyping analysis is indicated. Bar = 1 kb.

initiation codon and is disrupting the 5′ donor splicing site of the 6th intron. No additional T-DNAs are detected by DNA gel blot analysis. *serk2-2* was backcrossed with Columbia and the F2 progeny analyzed by segregation of the BASTA-resistant phenotype and by PCR-assisted genotyping. The results indicate that this T-DNA insertion line also represents a single insertion in the *SERK2* gene. The location of the *serk2-2* T-DNA insertion is presented in Figure 1B.

To determine whether the alleles identified are null mutants, RT-PCR was used to detect *SERK1* and *SERK2* transcripts in plants shown to be homozygous for the tagged alleles. *SERK1* transcripts could be detected in *serk1-1* (Figure 2A). The *serk1-1* mutant allele may therefore not represent a full knockout. A *SERK2* transcript containing sequences upstream of the T-DNA insertion can be detected (data not shown), but no *SERK2* transcripts downstream of the T-DNA insertion were observed in *serk2-2* mutant plants (Figure 2B). Because the truncated *SERK2* transcripts lack the entire *SERK2* kinase domain, we assume that the *serk2-2* allele is a null mutant.

In order to investigate whether the truncated *serk1-1* encodes a functional protein, we engineered a modified SERK1 kinase missing the last 90 amino acids corresponding to kinase subdomain XI and the C-terminal region. The SERK1^{kin} and deletion mutant SERK1$^{kin\Delta D536\text{-}R626}$ constructs were tested for kinase activity in vitro. Figure 2D shows that the SERK1$^{kin\Delta D536\text{-}R626}$ mutant protein no longer autophosphorylates, indicating that subdomain XI and the C-terminal region of the SERK1 protein are essential for kinase activity. We conclude that the *serk1-1* allele encodes a nonfunctional kinase.

The *serk1-1* and *serk2-2* T-DNA insertion alleles contain a single T-DNA insertion in the *SERK1* and *SERK2* genes. The homozygous *serk1-1*, *serk1-2*, and *serk2-2* single mutant plants are morphologically indistinguishable from wild-type plants, display normal growth and development, and are fully fertile (data not shown).

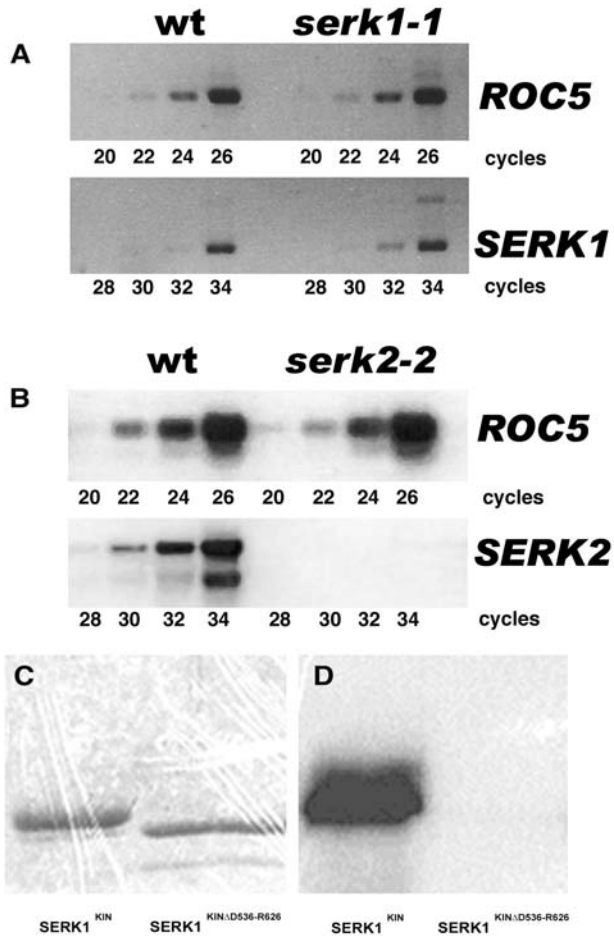

Figure 2. Molecular Analysis of *serk1-1* and *serk2-2* Mutant Alleles.

(A) Semiquantitative RT-PCR analysis of *SERK1* transcripts in the wild type and the *serk1-1* mutant.

(B) Semiquantitative RT-PCR analysis of *SERK2* transcripts in the wild type and the *serk2-2* mutant. The *ROC5* gene was amplified simultaneously as a control in both experiments.

(C) Bacterially produced SERK1^{kin} and SERK1$^{kin\Delta D536\text{-}R626}$ proteins were affinity purified and incubated with [γ-^{32}P]ATP. After separation on 10% SDS-PAGE, the resulting gels were stained with Coomassie blue.

(D) Same gels after autoradiography using a PhosphorImager.

SERK1 and SERK2 Expression Patterns Are Overlapping

Semiquantitative RT-PCR analysis was used to compare *SERK1* and *SERK2* expression in wild-type plants. Transcripts of *SERK1* and *SERK2* were most abundant in floral buds but were also present at a lower level in the different vegetative tissues (Figures 3 and 4A to 4F).

C-terminal fusions between SERK1 and yellow fluorescent protein (YFP) (Kwaaitaal et al., 2005) as well as SERK2 and YFP were expressed in *Arabidopsis* under control of their respective promoters. Fluorescent fusion protein localization was then followed in more detail during root and anther development by confocal microscopy. In the wild type, both the tapetum and the developing microspores up to and including the differentiation of the descendents of the second parietal division contain the SERK1 (Kwaaitaal et al., 2005; Figures 4B to 4E) and SERK2 proteins (Figures 4G to 4J). After that stage, both proteins are found to be specifically present in the membranes of the developing tapetal and middle cell layers. By the end of stage 5, the receptors are no longer found in meiocytes (Figures 4E and 4J). This pattern of fusion protein localization is in accordance with the mRNA in situ hybridization data presented by Colcombet et al. (2006), who report that the expression pattern of both genes is initially uniform and at stage 5 of anther development is restricted to the middle layer and tapetum tissues. However, we also observe SERK1-green fluorescent protein fusions at a low level in the endothecium and epidermal cell layers of the anther. These differences may be caused either by technical limitations or differences in the stability of the SERK1 and SERK2 mRNA compared with the respective proteins. Our results also confirm that SERK2 protein localization largely overlaps with that of SERK1. However, differences are noted: SERK2 proteins are more abundant in the root vasculature, while SERK1 proteins are more abundant in the epidermal cell layers of the root (Figures 4A and 4F). It remains to be determined whether these local changes in abundance have functional importance.

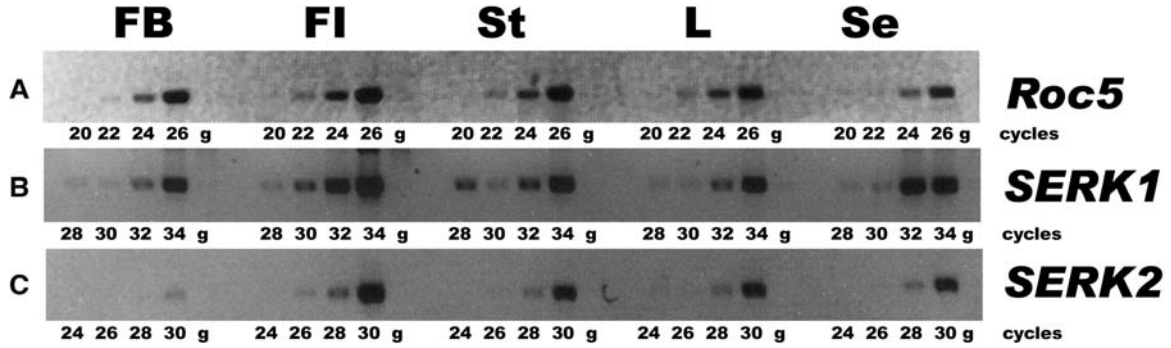

Figure 3. SERK1 and SERK2 Expression during Plant Development Determined by Semiquantitative RT-PCR.

(A) *ROC5* expression pattern.
(B) *SERK1* expression pattern.
(C) *SERK2* expression pattern.
''g'' is the control for genomic contamination and is performed on non-reverse-transcribed total RNA at 34 cycles for *SERK1*, 30 cycles for *SERK2*, and 26 cycles for *ROC5*. FB, flower buds; FI, opened flowers containing embryos from stage 0 through 7; St, stem; L, leaves; Se, seedlings 7 d after germination.

To determine whether the SERK1 and SERK2 proteins can indeed interact in cells that express both genes, we employed the transient assay in cowpea (*Vigna unguiculata*) protoplasts previously used to demonstrate that the SERK1 proteins can homodimerize (Shah et al., 2002). Using the fluorescence lifetime imaging microscopy (FLIM)–based system to detect fluorescence resonance energy transfer (FRET) (Russinova et al., 2004), we analyzed the properties of the SERK1 and SERK2 proteins fused to the spectral variants cyan fluorescent protein (CFP) and YFP, respectively, to form heterodimers. The results are shown in

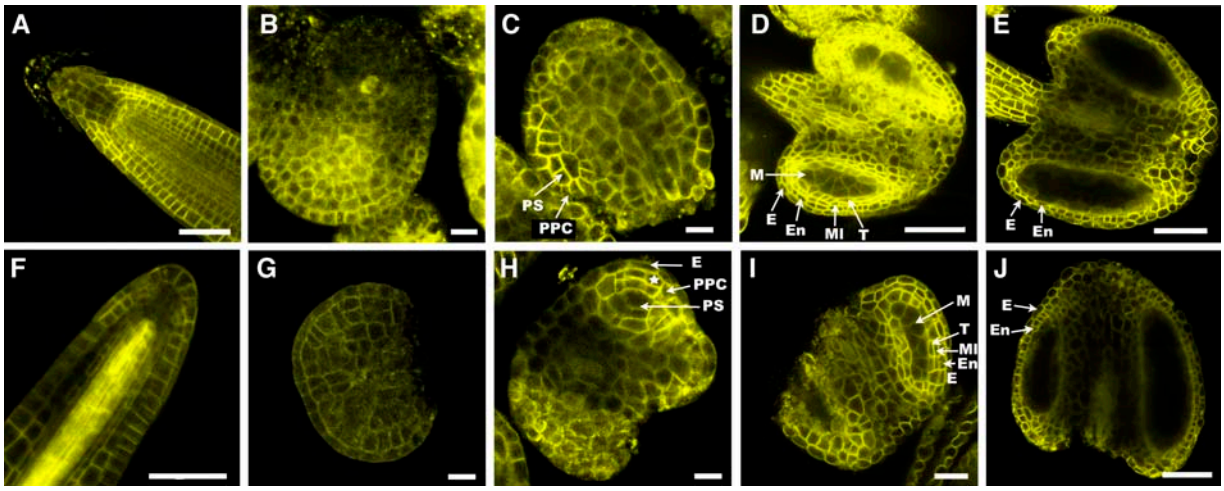

Figure 4. SERK1 and SERK2 Localization.

(A) SERK1 expression in root tip.
(B) SERK1 expression in anther primordial at stage 1.
(C) SERK1 expression in anther at stage 3.
(D) SERK1 expression in anther at stage 5.
(E) SERK1 expression in mature anther.
(F) SERK2 expression in root tip.
(G) SERK2 expression in anther primordial at stage 1.
(H) SERK2 expression in anther at stage 3.
(I) SERK1 expression in anther at stage 5.
(J) SERK2 expression in mature anther.
The star indicates cells of the preparietal cell layer that have divided to give rise to the outer and inner secondary parietal layers. PPC, preparietal cell layer; PS, primary sporogenous cell layer; E, epidermis; En, endothecium; MI, middle layer; M, meiocytes; T, tapetum. Bars = 50 μM for **(A)**, **(D)**, **(F)**, **(J)**, and **(E)**, 20 μM for **(I)**, and 10 μM for **(B)**, **(C)**, **(G)**, and **(H)**.

Figures 5A to 5F and clearly show that SERK1 and SERK2 can homodimerize as well as heterodimerize in the plasma membrane. We conclude that the overlapping expression pattern of the *SERK1* and *SERK2* genes, their subcellular localization in the plasma membrane, and the ability to form homodimers or heterodimers strongly suggest that the two genes can be acting together in the same complex and may be able to compensate for each other upon the loss of one.

The *serk1-1 serk2-2* Double Mutant Is Male Sterile

To answer whether functional redundancy between SERK1 and SERK2 may have obscured a possible defect in the alleles so far characterized, we generated and analyzed *serk1-1 serk2-2* double mutants.

The F2 progeny derived from a cross between homozygous *serk1-1* and *serk2-2* mutants was screened by PCR for the presence of *serk1-1 serk2-2* double mutants. When germinated on plates and grown on soil, all double mutants identified grow into normal plants and exhibit a normal vegetative development. The first visible defect is observed when flowers and siliques develop (Figures 6A and 6B). Although the double mutant plants develop normal inflorescence architecture and floral structures, they fail to form siliques. A closer inspection of the mutant flowers indicates that the floral organs develop normally within the closed bud, but the anther filaments do not elongate sufficiently to position the locules above the stigma at anthesis (Figures 6C and 6D). No pollen is released from the anthers in the double *serk1-1 serk2-2* mutant (Figures 6E and 6F). While the wild-type

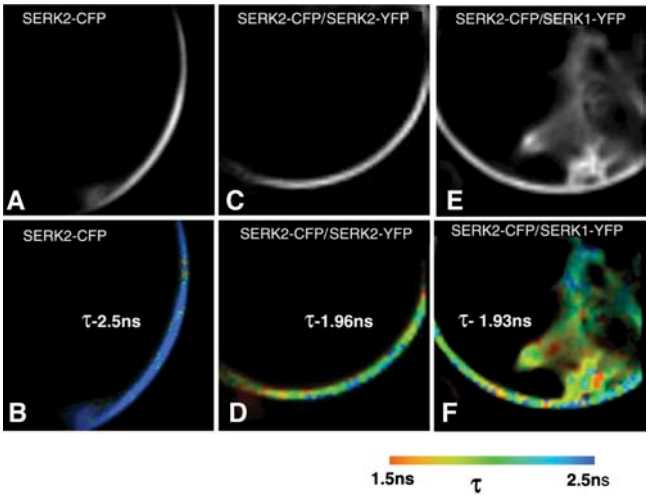

Figure 5. FRET between SERK1 and SERK2 Imaged by FLIM.

FLIM on cowpea protoplast transiently expressing SERK2-CFP (**[A]** and **[B]**) SERK2-CFP/SERK2-YFP (**[C]** and **[D]**), and SERK2-CFP/SERK1-YFP (**[E]** and **[F]**) for 16 h. Intensity images representing a steady state of the donor SERK2-CFP fluorescence are presented in **(A)**, **(C)**, and **(E)**. The mean fluorescence lifetime values (τ) and the lifetime distribution for the images in **(A)**, **(C)**, and **(E)** are presented as pseudocolor images in **(B)**, **(D)**, and **(F)**. Note the color bar where dark blue color is used to display $\tau = 2.5$ ns (no interaction) and the red to dark orange color to display $\tau = 1.5$ ns (interaction).

mature and immature anthers contained pollen grains and microspores, the double mutant anthers lacked both pollen and microspores. These characteristics are typical of a male sterility phenotype. The male sterility phenotype of the double mutant segregates as a Mendelian inherited recessive trait, suggesting that the observed defect is due to two sporophytically expressed genes. Only plants homozygous for both mutations show undeveloped siliques, indicating that the presence of one wild-type copy of either the *SERK1* or the *SERK2* gene is sufficient for pollen development.

The homozygous *serk1-1 serk2-2* mutant is completely female fertile and segregates 3:1 in the F2 generation of a backcross with either wild-type, *serk1-1*, or *serk2-2* pollen. The characterization of theses mutant alleles suggests that female gametogenesis is not dependent on signaling mediated by the SERK1-SERK2 combination.

To provide definite evidence that the observed phenotype is caused by the disruption of the *SERK1* and *SERK2* genes, we performed several complementation experiments. Transgenic lines were generated expressing the SERK1-YFP and SERK2-YFP proteins under control of their own promoters (P_{SERK1}:*SERK1-YFP* and P_{SERK2}:*SERK2-YFP* for the *SERK1* and *SERK2* transgenes, respectively) in a heterozygous *serk2-2 serk2-2 serk1-1* SERK1 background. The T1 seeds were selected by fluorescence under the binocular for the presence of the transgene. The selected T1 seeds were grown on media containing both kanamycin and BASTA. Resistant seeds were grown on soil and further genotyped by PCR-assisted genotyping. Among all T1 seeds selected, eight were *serk1-1 serk2-2* double mutant carrying the P_{SERK1}:*SERK1-YFP* transgene and three were *serk1-1 serk2-2* double mutant carrying the P_{SERK2}:*SERK2-YFP* transgene. All the T1 lines *serk1-1 serk2-2* double mutant carrying a transgene, whether P_{SERK1}:*SERK1-YFP* or P_{SERK2}:*SERK2-YFP* showed normal silique development and seed formation (Figures 6G to 6I). Eight T2 seeds of each characterized T1 line were further analyzed and confirmed to be *serk1-1 serk2-2* double mutant carrying a transgene, whether P_{SERK1}:*SERK1-YFP* or P_{SERK2}:*SERK2-YFP*. From these results, we conclude that the male sterility phenotype in the *serk1-1 serk2-2* double mutant is caused by the simultaneous disruption of the *SERK1* and the *SERK2* genes.

Microsporogenesis Arrests after Meiosis II, and the Tapetum Is Not Specified in *serk1-1 serk2-2* Mutants

To analyze in detail the developmental defects that cause male sterility in the double *serk1-1 serk2-2* mutant, we compared anther and pollen development in wild-type and double mutant plants.

Anther development has been divided into 14 stages based on morphological landmarks or cellular events visible under the light microscope (Goldberg et al., 1993; Sanders et al., 1999). The anther tissues derive from three germ layers designated L1, L2, and L3 that give rise to the epidermis, the archesporial cells, and the vascular tissue, respectively. At stage 3, the parietal cell layers and the sporogenous cells have been formed in wild-type anthers (Figure 7A) and in the *serk1-1 serk2-2* anthers (Figure 7B). In the *serk1-1 serk2-2* mutant, the two characteristic inner and

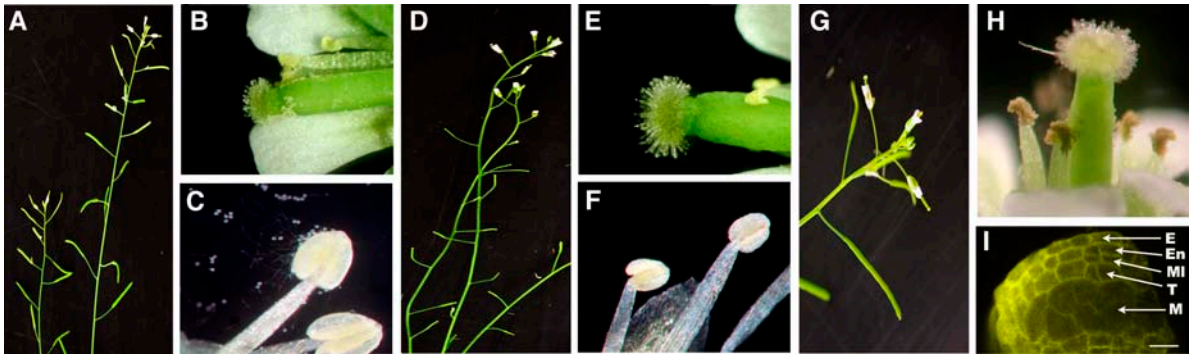

Figure 6. Phenotype of the *serk1-1 serk2-2* Double Mutant and the Complemented Mutant by the SERK1 cDNA-YFP Fusion Driven by the SERK1 Promoter (P_{SERK1}:*SERK1-YFP*).

(A) Inflorescence of a wild-type plant showing normal seed pods.
(B) A wild-type flower showing pollen grains.
(C) A wild-type anther showing germinating pollen grain.
(D) Inflorescence of the *serk1-1 serk2-2* double mutant with small seedpods and no developing seeds.
(E) A double *serk1-1 serk2-2* mutant flower with shortened anther filament and no pollen grain.
(F) A close-up of the double *serk1-1 serk2-2* mutant anther with no pollen grain.
(G) Plant from a complemented transgenic double *serk1-1 serk2-2* mutant showing normal seed pot.
(H) P_{SERK1}:*SERK1-YFP* complemented double mutant flower showing pollen grain.
(I) Anther of a P_{SERK1}:*SERK1-YFP* complemented double mutant visualized by confocal microscopy showing the five characteristic layers of an anther at stage 5. M, meiocytes; T, tapetum; MI, middle layer; En, endocethium; E, epidermis. Bar = 10 μm.

outer cortical cell layers surrounding the sporogenous cells are clearly visible, and no deviation from the wild-type development was observed up to stage 4 (Figures 7B and 7E). At stage 5, a wild-type anther is typically formed of five layers that are, from the outside to the inside, the epidermis, endothecium, middle layer, tapetum, and microsporocytes. The microsporocytes are located at the center of the locules and are larger than the tapetal cells and more rectangular in shape (Figure 7C). In the *serk1-1 serk2-2* mutant anther at stage 5, no tapetal layer can be identified. Instead, an increased number of microsporocytes is observed compared with the wild type (Figure 7F). At stage 6, the wild-type microsporocytes are isolated and detached from the tapetum layer and the middle layer degenerates (Figure 7G). In the double mutant anther, enlarged and undetached microsporocytes are observed (Figure 7J). At stage 7, cytokinesis in the wild-type anther is taking place, leading to the formation of tetrads (Figure 7H). In the double mutant anther, degenerating tetrads can be observed (Figure 7K). At stage 11, individual spores are released from the tetrads, and the tapetum layer degenerates in the wild-type anther (Figure 7I). In the double mutant, the cell debris of the collapsed microspores occupies the center of the locule and a highly vacuolated middle layer persists (Figure 7L).

To confirm that the anther of the *serk1-1 serk2-2* double mutant lacks a tapetal cell layer, we tested the expression of the *ARABIDOPSIS THALIANA ANTHER7* (*ATA7*) gene, an early tapetum marker (Rubinelli et al., 1998). *ATA7* is not expressed in the double *serk1-1 serk2-2* mutant, providing molecular evidence for the complete absence of tapetal layer specification in the double mutant (Figure 8).

We observed that in the double *serk1-1 serk2-2* mutant anther the tapetal cell layer is absent and an increased number of microsporocytes developed. One possibility is that the additional microsporocytes formed at stage 5 are derived from the inner secondary parietal layer. To test that hypothesis, we examined 51 and 61 locules of wild-type and mutant anthers, respectively, originating from three individual wild-type and double mutant plants. In wild-type anthers, the average number of microsporocytes and tapetal cells is 3.3 ± 0.7 and 10.2 ± 1.1, respectively. In the double mutant anther, the average number of microsporocytes is 9.7 ± 1.2. This number is close to the sum of microsporocytes and tapetal cells per wild-type locule. These results indicate that, in the double *serk1-1 serk2-2* mutant, cells that normally develop into tapetal cells may have acquired microsporocytic fate.

The transverse sections of the *serk1-1 serk2-2* double mutant anthers indicate that the differentiation of the meiocytes is abnormal starting from stage 6 onwards. To confirm that *serk1-1 serk2-2* meiocytes enter and proceed into meiosis, we followed the progression of meiosis in pollen mother cells derived from wild-type and double mutant plants. Wild-type and double mutant anther were therefore stained with propidium iodide and visualized using confocal microscopy. In wild-type male meiocytes, individual chromosomes are first detected at leptotene, when they start to condense and form granular and thread-like structures. Fully synapsed chromosomes can be visualized as looped ribbon-like structures also called pachytene chromosomes (Figure 9A). The five paired chromosomes align along the equator and can be detected as five bivalents at metaphase I. The homologues separate at anaphase I (Figure 9C), and five homologues migrate towards each opposite pole, leading to the formation of two groups of five partially decondensed chromosomes at telophase I. At metaphase II, 10 condensed chromosomes are clearly visible and are distributed equally to the two

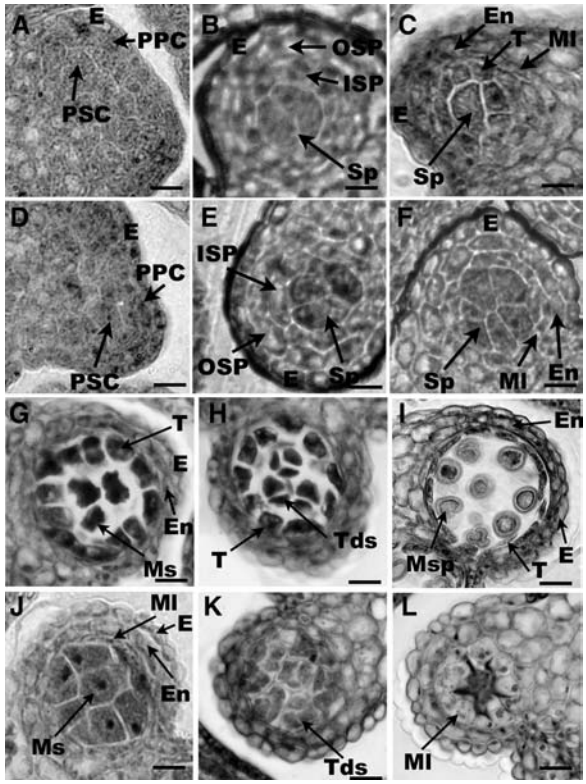

Figure 7. Anther Development in the Double *serk1-1 serk2-2* Mutant.

Micrographs of one of the four lobes of the wild type and double mutant stained with Toluidine blue. PPC, primary parietal cells; PSC, primary sporogenous cells; ISP, inner secondary parietal layer; OSP, outer secondary parietal layer; Sp, sporocytes; E, epidermis; En, endothecium; MI, middle layer; Ms, microsporocytes; Msp, microspores; T, tapetal layer; Tds, tetrads. Bars = 10 μm.

(A) Wild-type anther at stage 3 showing the inner primary sporogenous layer and the outer primary parietal layer.

(B) Wild-type anther at early stage 4 showing the inner and outer secondary parietal cell layer.

(C) Wild-type anther at late stage 5 showing the well organized four anther layers, the epidermis, the endothecium, the middle layer, and the tapetum and the sporocytes developing in the middle of the locule.

(D) *serk1-1 serk2-2* double mutant at stage 3 showing the inner primary sporogenous layer and the outer primary parietal layer.

(E) *serk1-1 serk2-2* double mutant anther at late stage 4 showing the two characteristic inner and outer secondary parietal cell layers.

(F) *serk1-1 serk2-2* double mutant anther at late stage 5 showing the absence of the tapetal layer and an aberrant number of microsporocytes.

(G) Wild-type anther at stage 6 showing isolated microsporocytes, highly vacuolated tapetum cells, a collapsing middle layer, the endocethium, and the epidermis.

(H) Wild-type anther at stage 7 with tetrads.

(I) Wild-type anther at stage 11 with pollen grains and degenerating tapetum.

(J) *serk1-1 serk2-2* double mutant anther at stage 6 showing enlarged and undetached microspores. The middle layer has not degenerated.

(K) *serk1-1 serk2-2* double mutant anther at stage 7 with degenerating tetrads.

(L) *serk1-1 serk2-2* double mutant anther at stage 11 showing the cell debris of the collapsed meiocytes and a persistent and highly vacuolated middle layer.

sides of the organelle band into two groups of five each. At anaphase II, the individual chromatids separate and move toward the spindle poles (Figure 9E). Finally, at telophase II, four groups of five chromatids are formed (Figure 9G). At the end of meiosis, the external and intersporal walls of the tetrad are dissolved to release individual microsporocytes by a mixture of enzymes collectively referred to as callase (Frankel et al., 1969). The individual microspores of the tetrad then initiate development of the pollen wall (Figure 9I).

We examined microsporocytes derived from the double mutant and found various stages of nuclear division, from prophase I to telophase II (Figures 9B, 9D, 9F, and 9H), suggesting that the meiotic nuclear divisions in the double *serk1-1 serk2-2* mutant was essentially normal. However, in *serk1-1 serk2-2* microsporocytes, the formed tetrads rapidly degenerate and disintegrate completely. Finally, there is a complete absence of pollen in the mature *serk1-1 serk2-2* flowers (Figures 9J and 9L).

The phenotypic data of the *serk1-1 serk2-2* mutant were all confirmed with the second independent allele *serk1-2* that we used to create the *serk1-2 serk2-2* double mutant (data not shown).

DISCUSSION

SERK1 and SERK2 Are Required for Tapetal Cell Fate and Microspore Formation

We report here that two members of the Arabidopsis LRR-RLK family, SERK1 and SERK2, are essential for male sporogenesis. In the *serk1-1 serk2-2* and *serk1-2 serk2-2* double mutants, the tapetal cells are not specified. By contrast, additional sporocytes are observed, suggesting that tapetal precursor cells can acquire a meiocyte fate in the absence of SERK1/SERK2-mediated signaling. The supernumerary mutant sporocytes enter and proceed into meiosis until the tetrad stage, after which the meiocytes degenerate, resulting in complete male sterility. These results indicate that SERK1 and SERK2 are required for normal

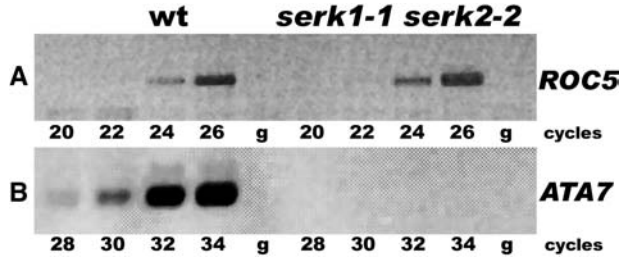

Figure 8. Expression of *ATA7* in the *serk1-1 serk2-2* Double Mutant.

ATA7, a tapetum-specific marker, is not expressed in the *serk1-1 serk2-2* double mutant. PCR products were collected after 28, 30, 32, and 34 cycles for *ATA7* and after 20, 22, 24, and 26 cycles for *ROC5*. "g" stands for the control on genomic contamination and is performed on non-reverse-transcribed total RNA at 34 cycles for *ATA7* and 26 cycles for *ROC5*.

(A) *ROC5* expression pattern.

(B) *ATA7* expression pattern.

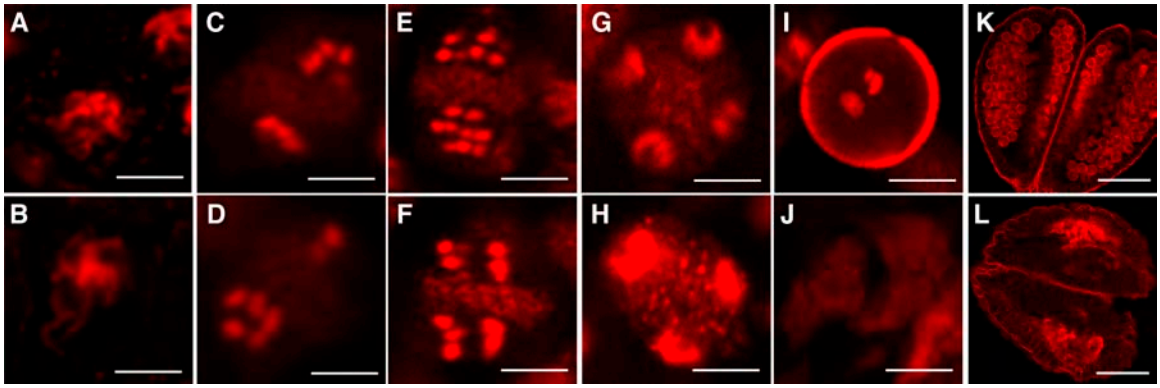

Figure 9. Male Meiosis in the *serk1-1 serk2-2* Double Mutant.

Micrographs of wild-type and *serk1-1 serk2-2* double mutant anthers stained with propidium iodide and viewed by confocal microscopy. Bars = 10 μm for **(A)** to **(J)** and 20 μm for **(K)** and **(L)**.
(A) Wild type pachytene chromosomes.
(B) *serk1-1 serk2-2* pachytene chromosomes.
(C) Wild-type anaphase I.
(D) *serk1-1 serk2-2* anaphase I.
(E) Wild-type anaphase II.
(F) *serk1-1 serk2-2* anaphase II.
(G) Wild-type telophase II.
(H) *serk1-1 serk2-2* telophase II.
(I) Wild-type pollen grain after mitosis I.
(J) *serk1-1 serk2-2* degenerated tetrads.
(K) Wild-type mature anther showing pollen grain.
(L) *serk1-1 serk2-2* collapsed anther.

meiotic cytokinesis and subsequent spore formation but have no apparent function in meiosis. Neither SERK1 nor SERK2 is expressed in the meiocytes at the stage of development in which the defect in the double mutant is observed. Instead, both proteins are present in tapetal cells in the wild type at the comparable stage. Hence, the observed failure to complete meiocyte cytokinesis in the double mutant is apparently the result of a previous defect in signaling between the sporocytes and the tapetal precursor cells.

In the *serk1-1 serk2-2* and *serk1-2 serk2-2* double mutants, the appearance of the developing meiocytes is different from their wild-type counterparts. Therefore, SERK1 and SERK2 might also be involved in meiocyte differentiation at the time of cytokinesis. We consider this unlikely due to the absence of expression of both genes in the wild-type meiocytes at this stage. The observed arrest in meiocyte cytokinesis in the double mutants is therefore more likely to be a consequence of the absence of the tapetal cell layer. In wild-type anthers, SERK1 and SERK2 proteins are highly expressed in the tapetal layer at the time of meiocyte cytokinesis.

The essential role of tapetal cells for pollen formation was demonstrated by ablation studies and genetic analysis. Ablation studies made use of genetic lasers in transgenic tobacco (*Nicotiana tabacum*) plants. A tapetum-specific promoter (*TA29*) was fused to several cytotoxic genes to selectively destroy the tapetum during anther development. These studies show that destruction of the tapetum by the cytotoxic gene led to the production of male-sterile plants (Koltunow et al., 1990; Mariani et al., 1990). These studies are further supported by the identification of mutants that are defective in tapetum development. For example, *ms1* and *ms3* mutations that cause abnormal vacuolation and enlargement of the tapetal cells also lead to defects in microspores (Chaudhury et al., 1994; Wilson et al., 2001; Ito and Shinozaki, 2002). These studies indicate that destruction of the tapetal layer or defects of tapetal cell formation result in the failure of pollen development. Tapetal cells are important for pollen formation because they provide callase and other proteins important for the release of microspores from the tetrad as well as chemicals important for the formation of pollen outer walls (Mepham, 1970; Izhar and Frankel, 1971; Stieglitz, 1977). Based on the phenotypic deviations observed in the double mutants, we therefore propose that SERK1 and SERK2 perform a fully interchangeable signaling role required for male sporogenesis. Expression of SERK1 was observed in the ovule, female gametophyte, early embryos, and vascular cells of seedling roots, hypocotyls, and leaves (Hecht et al., 2001; Kwaaitaal et al., 2005). The SERK2 protein has the same expression pattern (C. Albrecht, unpublished data), suggesting that SERK1 and SERK2 are playing other roles in these tissues besides their role in male sporogenesis.

SERK1, *SERK2*, and Other Tapetum Genes

Two genes with a phenotype very similar to the one reported for the *serk1-1 serk2-2* and *serk1-2 serk2-2* double mutants have been identified in *Arabidopsis*. The *EXS*/*EMS* gene encodes a different putative Ser/Thr LRR-RLK (Canales et al., 2002; Zhao

et al., 2002). *TPD1* encodes a putative secreted protein and is believed to be involved in the same signaling pathway (Yang et al., 2003). These two genes affect microspore formation as a result of the absence of a functional tapetal cell layer. In both the *exs/ems* and *tpd1* mutants, as well as in the *serk1-1 serk2-2* and *serk1-2 serk2-2* double mutants, the absence of the tapetal cell layer results in an increase of the number of meiocytes developed. The reciprocal effect was recently observed in mutants of the *MYB33* and *MYB65* genes, where the tapetum cells are seen to expand at the expense of the meiocytes, finally resulting in complete male sterility (Millar and Gubler, 2005). Apparently, reciprocal control between the gametophytic and the sporophytic tissues is required to maintain the appropriate balance between meiocyte and tapetum fate in order to finally develop fertile pollen. Recently, it was shown that the *AGAMOUS* transcriptional activator controls microspore development by activation of the *SPOROCYTELESS* (*SPL*) gene (Ito et al., 2004). The *SPL*/*NOZZLE* (*NZZ*) gene, a nuclear protein related to MADS box transcription factors, is required for archesporial specification (Schiefthaler et al., 1999; Yang et al., 1999). The *SPL* gene is expressed in the sporogenous cells and their descendants, the sporocytes. Yang et al. (1999) suggested that SPL/NZZ regulates the expression of genes necessary for sporocyte cell fate determination. They further suggested that a signal from developing sporocytes is necessary for proper differentiation and growth of the adjacent parietal cell layer. *SERK1-SERK2* as well as *EXS*/*EMS* and *TPD1* genes clearly act downstream of *SPL*/*NZZ* since meiocytes are being properly specified in the former mutant backgrounds. During anther development, the *SERK1*, *SERK2*, and *EXS*/*EMS* genes are expressed in the same parietal cells and their precursors. Thus, SERK1 and SERK2 proteins, perhaps together with EXS/EMS, may be involved in the perception of a signal from developing microsporocytes to immature tapetal cells, as proposed by Yang et al. (1999) for EXS/EMS. The *TPD1* gene encodes a putative secreted protein, is predominantly expressed in microsporocytes, and may represent the signal from developing microsporocytes to surrounding tapetal cells. There is molecular-genetic evidence that the *TDP1* and *EXS*/*EMS* genes are involved in the same pathway (Yang et al., 2005). While the *serk1-1 serk2-2* double mutant clearly phenocopies the *tpd1* and *exs/ems* mutants, it remains to be determined whether the SERK1 and SERK2 proteins also act in the TPD1-EXS/EMS pathway or are part of a separate signal transduction pathway.

Different explanations have been proposed for the phenotype of the *exs/ems* mutant. The observed absence of tapetum cells and overproliferation of meiocytes can be the result of a failure to assume the tapetum cell fate of the descendants of the inner secondary parietal cells and the adoption of a meiocyte fate (Zhao et al., 2002). Alternatively, the formation of extra meiocytes is proposed to result from a failure to restrict archesporial cell fate in *exs/ems* mutant anthers (Canales et al., 2002). Our data suggest a model that is close to that of Zhao et al. (2002). In wild-type

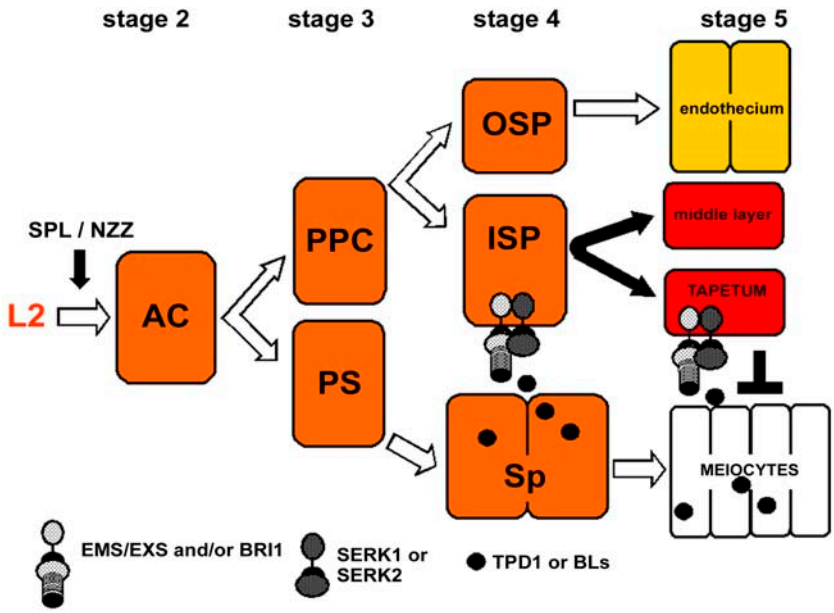

Figure 10. A Model for the SERK1-SERK2 Signaling Pathway in the Anther.

TDP1 and/or brassinosteroids produced in the developing meiocytes (Sp) signal the surrounding immature tapetal cells (ISP) through SERK1-SERK2/EMS-EXS or SERK1-SERK2/BRI1, respectively. Perception of the TPD1 and/or brassinosteroid signals ensures specification and maintenance of the tapetal and middle cell fate. One proposed function of the tapetum is to inhibit further proliferation of the meiocytes. In the *serk1-1 serk2-2* double mutant, specification of the tapetal cells does not occur. As a result, tapetal cells either adopt a meiocyte fate or the inner secondary parietal layer cells only form the middle layer. In both situations, formation of extra meiocytes occurs. Red-colored cells are expressing the SERK1 and SERK2 genes moderately (light red) or highly (dark red). Only anther stages 2 to 5 are represented. AC, archesporial cell; PPC, preparietal cell; PS, primary sporogenous cell layer; ISP, inner secondary parietal layer; OSP, outer secondary parietal layer; Sp, sporocyte; BLs, brassinosteroids.

anthers, SERK1/SERK2-mediated signaling can be employed to provide the tapetum fate to the inner descendants of the inner secondary parietal cells and could also be required for maintenance of the tapetum fate in stage 5. The tapetum cells then provide a second unknown signal to arrest multiplication of the stage 5 meiocytes. In *serk1-1/2 serk2-2* anthers, the observed extra meiocytes can then arise as proposed by Zhao et al. (2002) or from a series of extra cell divisions of the meiocytes. Presently, we have no evidence to support one or the other model for extra meiocyte formation. However, one can easily envisage the requirement of multiple, parallel signaling pathways involved in fate determination, maintenance, and proliferation in the developing anther (Figure 10).

SERK Genes Can Be Coreceptors in Multiple Receptor Kinase Complexes

While the expression of the *SERK1* and *SERK2* genes is fairly broad (Kwaaitaal et al., 2005), suggesting that both genes play a general role in plants, the phenotype of the *serk1-1 serk2-2* mutant is restricted to tapetal cells in the anther.

Previously, we reported that overexpression of the *SERK1* gene results in enhanced formation of embryogenic cells in tissue culture (Hecht et al., 2001). Comparing the formation of somatic embryos in culture of the *serk1-1* and *serk2-2* mutants using previously published protocols (Mordhorst et al., 1998) revealed no deviation from the wild type (C. Albrecht and S.C. de Vries, unpublished data). This suggested that there is redundancy in the proposed function of SERK1 in embryogenic cell formation in culture. We cannot exclude that this is due to the presence of the other member of the family due to the difficulty of molecularly characterizing homozygous double *serk1-1 serk2-2* immature mutant embryos and seedlings simultaneously with testing their embryogenic potential in culture. *serk1-1 serk2-2* mutants show no visible alteration in embryo development, suggesting functional redundancy of other SERK receptors during embryo development.

As shown for the ERECTA family RLKs (Shpak et al., 2003), tissue-specific and redundant expression of functionally equivalent SERK receptors might play a regulatory role in different aspects of plant development. The *SERK3/BAK1* gene has been identified as the coreceptor of *BRI1* (Li et al., 2002; Nam and Li, 2002). The *serk3/bak1* mutant phenotype is weaker than *bri1*, suggesting that SERK3 controls only a subset of the BRI1-mediated effects. Other *SERK* genes are therefore good candidates to mediate other elements of BRI1 signaling. Among the many phenotypic defects observed in strong *bri1* mutant alleles is male sterility, although the defects have not been investigated in detail (Clouse et al., 1996). Brassinosteroids were actually first isolated from pollen extracts, where they are produced in massive amounts (Grove et al., 1979). It is therefore tempting to speculate that SERK1 and SERK2, being close homologs of SERK3, can mediate BRI1 as well as EXS/EMS-mediated signaling during anther development. BRI1 and BRL1 proteins have significant similarity to the EXS/EMS receptor (Zhou et al., 2004). An attractive scenario could therefore be that the SERK1 and SERK2 proteins act as coreceptors of the EXS/EMS receptor kinase in the anther and perhaps as coreceptors of other receptors, such as BRI1, in other tissues as well as in anthers (Figure 10). This may represent an analogous situation to, for example, the TGFβ complexes in animal cells where the presence of particular main receptors in combination with coreceptors defines the ability of the cell to respond to various ligands (Di Guglielmo et al., 2003; Gonzáles-Gaitán, 2003).

METHODS

Plant Materials and Growth Conditions

The *Arabidopsis thaliana* Columbia ecotype was used as wild-type parent throughout. Seeds were surface sterilized, chilled at 4°C for 2 d, and then germinated and grown on plant growth Murashige and Skoog medium (Murashige and Skoog, 1962) supplemented with 1% sucrose at 22°C under a 16-h-light/8-h-dark photoperiod. One or two weeks after germination, seedlings were transferred to soil and grown to maturity in the same temperature and light conditions. The antibiotic plate assays were performed by supplementing the Murashige and Skoog medium with 25 mg·L^{-1} kanamycin or 15 mg·L^{-1} BASTA.

RT-PCR Analysis and Primers Used

RNA isolation, cDNA synthesis, and RT-PCR were performed as described by Hecht et al. (2001). For the detection of the *SERK1* and *SERK2* transcripts in their respective mutant backgrounds, cDNA synthesis was performed using random hexamer primers (Amersham Biosciences) instead of oligo(dT) primers. PCR products were collected after various cycles depending on the transcript amplified; the number of cycles used for each transcript is indicated in the figure. For the SERK1 and SERK2 expression patterns, the primer combinations used were V3 and S1utr3′ for *SERK1*, GSP4 and GSP1 for *SERK2*, and ATA7f and ATA7r for *ATA7*. The *cyclophilin ROC5* gene constitutively expressed was used as control, and the primers specific for this gene were ROC5-5 and ROC5-3. For the detection of the *SERK1* and *SERK2* transcripts in their respective mutant backgrounds, the primers used were V2 and S3 for *SERK1* and S2-K2 and GSP3 for *SERK2*. The primers used in this study are as follows: P2F (5′-TTTTGTTGAATTCACAATCTCTGCACC-3′); P2-NcoR (5′-CCCCATGGACCAAAAAAAAGCAAATTTCTCCTCCC-3′); P1F (5′-CTATGTGGCGAAAACTCACTTAATCTG-3′); P1-NcoR (5′-CGACTCCATGGCAAACAACAATGCTAAATTTCG-3′); GSP4 (5′-GATCTGGGAGGAGAAATTTGC-3′); Tag1R (5′-TGTTGCCGGTCTTGCGATGATTAT-3′); GSP1 (5′-CGGCTAGTAACTGGGCCGCATAGATCC-3′); S1utr3′ (5′-CCCTTTTAATCGAACCATAGCAC-3′); LB1 (5′-GCCTTTTCAGAAATGGATAAATAGCCTTGCTTCC-3′); S1-NcoF (5′-CGACTCCATGGAGTCGAGTTATGTGGTG-3′); S1-NcoR (5′-CGACTCCATGGCCTTGGACCAGATAACTCAACGGCG-3′); S2-NcoF (5′-CGACTCCATGGGGAGAAAAAAGTTTGAAGC-3′); S2-NcoR (5′-CGACTCCATGGTCTTGGACCAGACAACTCCATAGC-3′); V3 (5′-CGTGACAACAGCAGTCCGTGGCACCATCGG-3′); ROC5-5 (5′-TCTCTCTTCCAAATCTCC-3′); ROC5-3 (5′-AAGTCTCTCACTTTCTCACT-3′); YFPr (5′-CGATGGGGGTGTTCTGCTGGTAGT-3′); S2-K2K1 (5′-AGACAGCAAATCGCGCTAGG-3′); ATA7f (5′-AGACAGCAAATCGCGCTAGG-3′); ATA7r (5′-ATTTCTCAACGTCGGGATTCT-3′); *Sma*I1000 (5′-TCCCCCGGGTATTTTCTTCGATGTCCCTG-3′); BE-*Not*IR1785R (5′-AAGGAAAAAAGCGGCCGCCCACTAACATCTCTAGCTTC-3′); *Not*I2068 (5′-ATAAGAATGCGGCCGCCCTTGGACCAGATA-3′); V2 (5′-GCTGCTCCTGCAATAGCCTTTGCTTGGTGG-3′); S3 (5′-AGAGATATTCTGGAGCGATGTGACCGATGG-3′); S2-K2 (5′-ACCCTGAGGTTCACTTGGG-3′); GSP3 (5′-GTTAGGCAAATTACAATGTCG-3′).

Molecular Analysis of Single and Double Mutants

The *serk1* insertion lines (nr 044330 for *serk1-1* and nr 053021 for *serk1-2*) were obtained from the SIGnAL TDNA-Express collection (kanamycin

resistance) (Alonso et al., 2003) and the *serk2-2* insertion line (nr 119-G03) from the SAIL lines (BASTA or DL-phosphinothricin resistance) (Sessions et al., 2002). The PCR primers used for screening were V3 and S1utr3′ for *SERK1*, GSP4 and GSP1 for *SERK2*, and Tag1R and LB1 for the primers designed on the T-DNA insertion in the *SERK1* and *SERK2* genes, respectively. PCR screening employed a three primer PCR strategy that identified wild-type, heterozygous, and homozygous individuals in a single step using two gene-specific primers and one primer designed on the T-DNA. T-DNA insertion sites were determined by sequencing the PCR fragments. *serk1-1*, *serk1-2*, and *serk2-2* were backcrossed once with Columbia wild-type plants. The segregation of the F2 progeny was followed both by PCR-based genotyping and by the antibiotic plate assay. The *serk1-1* and *serk1-2* alleles were crossed with the *serk2-2* insertion line to generate the double *serk1-1 serk2-2* and *serk1-2 serk2-2* mutants. The F1 were allowed to self-fertilize, and candidate double mutant F2 plants were genotyped by a combination of PCR genotyping and antibiotic plate assays.

Genetic Complementation and Plasmid Generation

The entire open reading frame of *SERK1* and *SERK2* cDNAs was amplified by PCR from *SERK1* and *SERK2* full-length cDNAs (accession numbers A67827 and AF384969, respectively). The forward and reverse primers were engineered with an *Nco*I site to replace the *SERK1* and *SERK2* stop codons and allow an in-frame fusion with YFP. The primers used were S1-NcoF and S1-NcoR for the *SERK1* cDNA and S2-NcoF and S2-NcoR for the *SERK2* cDNA.

To prepare the *SERK1* and *SERK2* promoter constructs, a 2-kb region upstream of the start codons of the *SERK1* and *SERK2* genes was amplified from Columbia genomic DNA and cloned in the PGEM-T vector (Promega). The primers used were P1F and P1-NcoR for the *SERK1* promoter and P2F and P2-NcoR for the *SERK2* promoter. The PGEM-T cloned promoters were inserted via *Sal*I-*Nco*I in a modified pBluescript SK+ vector containing the YFP gene inserted as *Nco*I-*Bam*H1 fragment in front of the Tnos terminator. The entire open reading frames of *SERK1* and *SERK2* as described above were then inserted as *Nco*I fragments. The resulting full cassettes were then subcloned into a modified pFluar vector via *Sal*I-*Sma*I (Stuitje et al., 2003). These constructs will be further referred as P_{SERK1}:*SERK1-YFP* and P_{SERK2}:*SERK2-YFP* for the *SERK1* and *SERK2* transgenes, respectively.

These constructs were verified by sequencing and were electroporated in *Agrobacterium tumefaciens* strain C58C1 containing a disarmed C58 Ti plasmid (Koncz et al., 1989). *Arabidopsis* plants homozygote mutant for the *serk2-2* locus and heterozygote for the *serk1-1* locus were transformed by the floral dip method as described by Clough and Bent (1998). Fluorescent T1 seeds were selected with a stereomicroscope using a DsRed filter. The selected T1 seeds were selected on plates containing both kanamycin and BASTA. The resistant seedlings were transferred to soil and analyzed by PCR-assisted genotyping to identify the *serk1-1 serk2-2* double mutant harboring the transgene. The primers used for the identification of the double *serk1-1 serk2-2* mutant were as previously described. The primers used for the detection of the transgene were V3 and YFPr for the *SERK1* transgene and S2-K2K1 and YFPr for the *SERK2* transgene.

SERK1 Kinase Constructs

The cDNA sequence encoding the SERK1 kinase catalytic domain, corresponding to nucleotides 1000 to 2068, was amplified by PCR using *SERK1* cDNA clone (accession number A67827; Hecht et al., 2001) as template. The primers used had tailored restriction sites and were *Sma*I1000 and *Not*I2068. The PCR fragment was digested by *Sma*I and *Not*I, purified, and cloned into pGEX-4T1 (Pharmacia), resulting in SERK1^{kin} construct. The SERK1 deletion mutant was obtained by PCR amplification using primers *Sma*I1000 and BE-*Not*IR1785R, located 40 bp downstream of the T-DNA insertion in the *serk1-1* allele. PCR fragments were digested by *Sma*I and *Not*I and cloned into pGEX-4T1, resulting in SERK1$^{kin\Delta D536\text{-}R626}$ construct. These constructs were verified by sequencing.

Kinase Assays

Glutathione *S*-transferase fusion proteins were purified according to the manufacturer's instructions as previously described (Shah et al., 2001). The kinase activity of the purified proteins was demonstrated by incubation for 30 min at 30°C of 500 ng of protein in 30-μL reaction mixture (20 mM Tris, pH 7.5, 50 mM NaCl, 0.01% Triton X-100, 1 mM DTT, 10 mM $MgCl_2$, 50 μM unlabelled ATP, and 10 μCi [γ-^{32}P]ATP). The reaction was stopped by adding Laemmli SDS-PAGE sample buffer, boiled at 95°C for 5 min, and separated by 10% SDS-PAGE. The gel was stained with Coomassie Brilliant Blue to verify equal loading and dried. The radioactivity was quantified with a PhosphorImager using the ImageQuant program (Molecular Dynamics).

Microscopy and Histological Staining

For the anther structure study, inflorescences of the wild type and the *serk1-1 serk2-2* double mutant were fixed in 5% glutaraldehyde in 25 mM sodium phosphate, pH 7.4, dehydrated in ethanol series to 95%, and embedded in Technovit 7100 according to the recommendations of the manufacturer (Heraeus Kulzer). Sections (7 μm) were prepared and stained with 0.25% of Toluidine blue.

Meiosis in wild-type and double *serk1-1 serk2-2* mutant plants was analyzed by confocal microscopy, as essentially described by Peirson et al. (1997). Inflorescences of wild-type and double mutant plants were fixed overnight in acetic acid:ethanol (1:3) solution. The fixed material was then incubated in 10 mM Tris, pH 8, containing 10 mM NaCl, 1% Triton X-100 (v/v), and 0.2 μg/mL propidium iodide for DNA staining. After washing in Tris buffer, the flower buds were dissected under the binocular before observation. Samples were viewed with a Zeiss confocal microscope (Axiovert 100M equipped with an LSM510 argon laser with a 543-nm laser line). Propidium iodide fluorescence was imaged using the following settings: 543-nm laser → HFT488/543 → sample → HFT488/543 → mirror → BP560-615 → detector.

Fluorescence Microscopy

Anthers and root apices from transgenic plants harboring P_{SERK1}:*SERK1-YFP* or P_{SERK2}:*SERK2-YFP* transgenes were used for confocal analyses. Transgenic roots and anthers were analyzed using a Zeiss confocal microscope (Axiovert 100M equipped with an LSM510 argon laser with a 514-nm laser line). YFP fluorescence was imaged using the following settings: 514-nm laser → HFT458/514 → sample → HFT458/514 → NFT635vis → BP535-590 → detector. Bright field was imaged using the following settings: 514-nm laser → HFT458/514 → sample → bright field. Autofluorescence spectral bleed-through was assessed by imaging at the same time with the YFP channel a channel that detects red fluorescence: 514-nm laser → HFT458/514 → sample → NFT635vis → LP650 → detector. The pinhole was adjusted for each channel in such a way that Z-resolution is equal (typically 2 μm). Amplifier gain for YFP and autofluorescence/spectral bleed-through channels are always set equal.

Transient Expression in Protoplasts

Cowpea (*Vigna unguiculata*) mesophyll protoplasts were prepared and transfected as previously described by Russinova et al. (2004).

FLIM

FLIM was performed using a Bio-Rad Radiance 2100 MP system in combination with a Nikon TE 300 inverted microscope. Two-photon

excitation pulses were generated by a Ti:sapphire laser (Coherent Mira) that was pumped by a 5-W Coherent Verdi laser. Pulse trains of 76 MHz (150-fs pulse duration; 860-nm center wavelength) were produced. The excitation light was directly coupled into the microscope and focused into the sample using a CFI Plan Apochromat ×60 water immersion objective lens (numerical aperture 1.2). Fluorescent light was detected using the nondescanned single photon counting detection, which is the most sensitive solution for two-photon imaging. For the FLIM experiment, the Hamamatsu R3809U multichannel plate photomultiplier tube was used, which has a typical time resolution of ~50 ps. CFP emission was selected using a 480DF 30-nm band-pass filter. Images with a frame size of 64 × 64 pixels were acquired, and the average count rate was 2.10^4 photons/s, for an acquisition time of 90 s (Borst et al., 2003; Chen et al., 2003; Becker et al., 2004; Chen and Periasamy, 2004). From the intensity images obtained, complete fluorescence lifetime decays were calculated per pixel and fitted using a double exponential decay model. The fluorescence lifetime of one component was fixed to the value found for SERK1-CFP (2.5 ns). The FRET efficiency (E) was determined by $E = 1 - \tau_{DA}/\tau_D$, where τ_D is the fluorescence lifetime of the donor in the absence of acceptor and τ_{DA} that of the donor in the presence of acceptor at a distance (R). The distance between the donor and the acceptor was determined from the relation $\tau_{DA} = \tau_D/(1 + (R_0/R)^6)$, where R_0 is the Förster radius, the distance between the donor and acceptor at which 50% energy transfer takes place (Elangovan et al., 2002).

Accession Numbers

Sequence data and seed stocks from this article can be found in the GenBank/EMBL data libraries under the following accession numbers: *SERK1* cDNA clone (A67827, At1g71830) and *SERK2* cDNA clone (AF384969, At1g34210). The *serk1-1* insertion lines were obtained from the SIGnAL TDNA-Express collection, with the accession numbers 044330 and 053021. The *serk2-2* insertion line was obtained from the SAIL lines, with the accession number 119-G03.

ACKNOWLEDGMENTS

We thank Jan-Willem Borst (Wageningen University) for help with FLIM, Olga Kulikova (Wageningen University) for help with microscopical analysis, Boudewijn van Veen (Wageningen University) for help in editing and formatting the images shown in this article, and the Nottingham Arabidopsis Stock Centre for supplying the Salk insertion seed and SAIL lines. This work was supported by the Agrotechnology and Food Sciences Group of Wageningen University (C.A., E.R., and S.d.V.), by Grant ERBIO4-CT96-0689 from the European Union Biotechnology Program (V.H.), and by Grant QLG2-2000-00602 from the European Union Quality of Life and Management of Living Resources Program (E.R.).

Received August 4, 2005; revised October 5, 2005; accepted October 18, 2005; published November 11, 2005.

REFERENCES

Alonso, J.M., et al. (2003). Genome-wide insertional mutagenesis of *Arabidopsis thaliana.* Science **301,** 653–657.

Becker, W., Bergmann, A., Hink, M.A., Konig, K., Benndorf, K., and Biscup, C. (2004). Fluorescence lifetime imaging by time-correlated single-photon counting. Microsc. Res. Tech. **63,** 58–66.

Bicknell, R.A., and Koltunow, A.M. (2004). Understanding apomixis: Recent advances and remaining conundrums. Plant Cell **16** (suppl.), S228–S245.

Borst, J.W., Hink, M., van Hoek, A., and Visser, A.J.W.G. (2003). Multiphoton microspectroscopy in living plant cells. In Multiphoton Microscopy in the Biomedical Sciences III, A. Periasamy and P.T. So, eds (Bellingham, WA: SPIE), pp. 231–238.

Canales, C., Bhatt, A.M., Scott, R., and Dickinson, H. (2002). *EXS*, a putative LRR receptor kinase, regulates male germline cell number and tapetal identity and promotes seed development in Arabidopsis. Curr. Biol. **12,** 1718–1727.

Caño-Delgado, A., Yin, Y., Yu, C., Vafeados, D., Mora-Garcia, S., Cheng, J.-C., Nam, K.H., and Chory, J. (2004). BRL1 and BRL3 are novel brassinosteroid receptors that function in vascular differentiation in *Arabidopsis.* Development **131,** 5341–5351.

Chaudhury, A.M., Lavithis, M., Taylor, P.E., Craig, S., Singh, M.B., Signer, E.R., Knox, R.B., and Dennis, E.S. (1994). Genetic control of male fertility in *Arabidopsis thaliana*: Structural analysis of premeiotic developmental mutants. Sex. Plant Reprod. **7,** 17–28.

Chen, Y., Mills, J.D., and Periasamy, A. (2003). Protein localization in living cells and tissues using FRET and FLIM. Differentiation **71,** 528–541.

Chen, Y., and Periasamy, A. (2004). Characterization of two-photon excitation fluorescence lifetime imaging microscopy for protein localization. Microsc. Res. Tech. **63,** 72–80.

Clough, S.J., and Bent, A.F. (1998). Floral dip: A simplified method for *Agrobacterium*-mediated transformation in *Arabidopsis thaliana.* Plant J. **16,** 735–743.

Clouse, S.D., Langford, M., and McMorris, T.C. (1996). A brassinosteroid-insensitive mutant in *Arabidopsis thaliana* exhibits multiple defects in growth and development. Plant Physiol. **111,** 671–678.

Colcombet, J., Boisson-Dernier, A., Ros-Palau, R., Vera, C.E., and Schroeder, J.I. (2005). *Arabidopsis* SOMATIC EMBRYOGENESIS RECEPTOR KINASES1 and 2 are essential for tapetum development and microspore maturation. Plant Cell **17,** 3350–3361.

Di Guglielmo, G.M., Le Roy, C., Goodfellow, A.F., and Wrana, J.L. (2003). Distinct endocytic pathways regulate TGF-β receptor signalling and turnover. Nat. Cell Biol. **5,** 410–421.

Elangovan, M., Day, R.N., and Periasamy, A. (2002). Nanosecond fluorescence resonance energy transfer-fluorescence lifetime imaging microscopy to localize the protein interactions in a single living cell. J. Microsc. **205,** 3–14.

Frankel, R., Izhar, S., and Nitsan, J. (1969). Timing of callase activity and cytoplasmic male sterility in Petunia. Biochem. Genet. **3,** 451–455.

Goldberg, R.B., Beals, T.P., and Sanders, P.M. (1993). Anther development: Basic principles and practical applications. Plant Cell **5,** 1217–1229.

Gonzáles-Gaitán, M. (2003). Signal dispersal and transduction through the endocytic pathway. Nat. Rev. Mol. Cell Biol. **4,** 213–224.

Grove, M.D., Spencer, G.F., and Rehvedder, W.K. (1979). Brassinolide, a plant growth-promoting steroid isolated from *Brassica napus* pollen. Nature **281,** 216–217.

Hanks, S.K., Quinn, A.M., and Hunter, T. (1988). The protein kinase family: Conserved features and deduced phylogeny of the catalytic domains. Science **241,** 42–52.

Hecht, V., Vielle-Calzada, J.P., von Recklinghausen, I., Hartog, M., Zwartjes, C., Schmidt, E., Boutilier, K., Grossniklaus, U., and de Vries, S. (2001). The Arabidopsis *SOMATIC EMBRYOGENESIS RECEPTOR KINASE 1* gene is expressed in developing ovules and embryos and enhances embryogenic competence in culture. Plant Physiol. **127,** 803–816.

Ito, T., and Shinozaki, K. (2002). The *MALE STERILITY 1* gene of Arabidopsis, encoding a protein with a PHD-finger motif, is expressed in the tapetal cells and is required for pollen maturation. Plant Cell Physiol. **43,** 1285–1292.

Ito, T., Wellmer, F., Yu, H., Das, P., Ito, N., Alves-Ferreira, M., Riechmann, J.L., and Meyerowitz, E.M. (2004). The homeotic protein AGAMOUS controls microsporogenesis by regulation of SPOROCYTELESS. Nature **430,** 356–360.

Izhar, S., and Frankel, R. (1971). Mechanism of male sterility in Petunia: The relationship between pH, callase activity in the anthers, and the breakdown of the microsporogenesis. Theor. Appl. Genet. **44,** 104–108.

Kinoshita, T., Caño-Delgado, A., Seto, H., Hiranuma, S., Fujioka, S., Yoshida, S., and Chory, J. (2005). Binding of brassinosteroids to the extracellular domain of plant receptor kinase BRI1. Nature **433,** 167–171.

Koltunow, A.M., Truettner, J., Cox, K.H., Wallroth, M., and Goldberg, R.B. (1990). Different temporal and spatial gene expression patterns occur during anther development. Plant Cell **2,** 1201–1224.

Koncz, C., Martini, N., Mayerhofer, R., Koncz-Kalman, Z., Korber, H., Redei, J.P., and Schell, J. (1989). High-frequency T-DNA-mediated gene tagging in plants. Proc. Natl. Acad. Sci. USA **86,** 8467–8471.

Kwaaitaal, M., de Vries, S.C., and Russinova, E. (2005). The Arabidopsis Somatic Embryogenesis Receptor Kinase 1 protein undergoes endocytosis and is present in sporophytic and gametophytic cells. Protoplasma **226,** 55–65.

Li, J., Wen, J.Q., Lease, K.A., Doke, J.T., Tax, F.E., and Walker, J.C. (2002). BAK1, an Arabidopsis LRR receptor-like protein kinase, interacts with BRI1 and modulates brassinosteroid signaling. Cell **110,** 213–222.

Mariani, C., Beuckeleer, M.D., Truettner, J., Leemans, J., and Goldberg, R.B. (1990). Induction of male sterility in plants by a chimaeric ribonuclease gene. Nature **347,** 384–387.

Mepham, R.M. (1970). Development of pollen grain wall: Further work with *Tradescantia bracteata.* Protoplasma **68,** 39–54.

Millar, A.A., and Gubler, F. (2005). The Arabidopsis *GAMYB-like* genes, *MYB33* and *MYB65*, are microRNA-regulated genes that redundantly facilitate anther development. Plant Cell **17,** 705–721.

Mordhorst, A., Charbit, E., and de Vries, S.C. (2005). Somatic embryogenesis. In Plant Development and Biotechnology, R. Trigiano and R. Gray, eds (Boca Raton, FL: CRC Press), pp. 201–209.

Mordhorst, A.P., Toonen, M.A.J., and de Vries, S.C. (1997). Plant embryogenesis. CRC Crit. Rev. Plant Sci. **16,** 535–576.

Mordhorst, A.P., Voerman, K.J., Hartog, M.V., Meijer, E.A., van Went, J., Koornneef, M., and de Vries, S.C. (1998). Somatic embryogenesis in *Arabidopsis thaliana* is facilitated by mutations in genes repressing excess meristematic cell divisions. Genetics **149,** 549–563.

Murashige, T., and Skoog, F. (1962). A revised medium for rapid growth and bioassays with tobacco tissue culture. Plant Physiol. **15,** 473–497.

Nam, K.H., and Li, J. (2002). BRI1/BAK1, a receptor kinase pair mediating brassinosteroid signaling. Cell **110,** 203–212.

Peirson, B.N., Bowling, S.E., and Makaroff, C.A. (1997). A defect in synapsis causes male sterility in a T-DNA-tagged *Arabidopsis thaliana* mutant. Plant J. **11,** 659–669.

Reinert, J. (1959). Über die kontrolle der morphogenese und die induktion von adventivembryonen in gewebekulturen aus karotten. Planta **53,** 318–333.

Rubinelli, P., Hu, Y., and Ma, H. (1998). Identification, sequence analysis and expression studies of novel anther-specific genes of *Arabidopsis thaliana.* Plant Mol. Biol. **37,** 607–619.

Russinova, E., Borst, J.W., Kwaaitaal, M., Yanhai Yin, Y., Caño-Delgado, A., Chory, J., and de Vries, S.C. (2004). Heterodimerization and endocytosis of Arabidopsis brassinosteroid receptors BRI1 and SERK3 (BAK1). Plant Cell **16,** 3216–3229.

Sanders, P.M., Anhthu, Q.B., Weterings, K., McIntire, K.N., Hsu, Y., Lee, P.Y., Troung, M.T., Beals, T.P., and Goldberg, R.B. (1999). Anther developmental defects in *Arabidopsis thaliana* male sterile mutants. Sex. Plant Reprod. **11,** 297–322.

Schiefthaler, U., Balasubramatan, S., Sieber, P., Chevalier, D., Wisman, E., and Schneitz, K. (1999). Molecular analysis of *NOZZLE*, a gene involved in pattern formation and early sporogenesis during sex organ development in *Arabidopsis thaliana.* Proc. Natl. Acad. Sci. USA **96,** 11664–11669.

Schmidt, E.D.L., Guzzo, F., Toonen, M.A.J., and de Vries, S.C. (1997). A leucine-rich receptor-like kinase marks somatic plant cells competent to form embryos. Development **124,** 2049–2062.

Sessions, A., et al. (2002). A high-throughput Arabidopsis reverse genetics system. Plant Cell **14,** 2985–2994.

Shah, K., Russinova, E., Gadella, T.W. Jr, Willemse, J., and de Vries, S.C. (2002). The *Arabidopsis* kinase-associated protein phosphatase controls internalization of the somatic embryogenesis receptor kinase 1. Genes Dev **16,** 1707–1720.

Shah, K., Vervoort, J., and de Vries, S.C. (2001). Autophosphorylation properties of AtSERK1, a receptor-like kinase from *Arabidopsis thaliana.* J. Biol. Chem. **276,** 41263–41269.

Shiu, S.H., and Bleecker, A.B. (2001). Receptor-like kinases from Arabidopsis form a monophyletic gene family related to animal receptor kinases. Proc. Natl. Acad. Sci. USA **98,** 10763–10768.

Shpak, E.D., Berthiaume, C.T., Hill, E.J., and Torii, K.U. (2003). Synergistic interaction of three ERECTA-family receptor-like kinases controls *Arabidopsis* organ growth and flower development by promoting cell proliferation. Development **131,** 1491–1501.

Stieglitz, H. (1977). Role of β-1,3-glucan in postmeiotic microspore release. Dev. Biol. **57,** 87–97.

Stuitje, A.R., Verbree, E.C., van der Linden, K.H., Mietkiewska, E.M., Nap, J.-P., and Kneppers, T.J.A. (2003). Seed-expressed fluorescent proteins as versatile tools for easy (co)transformation and high-throughput functional genomics in *Arabidopsis.* Plant Biotechnol. J. **1,** 301–309.

Wilson, Z.A., Morroll, S.M., Dawson, J., Swarup, R., and Tighe, P.J. (2001). The Arabidopsis MALE STERILITY 1 (MS1) gene is a transcriptionnal regulator of male gametogenesis, with homology to the PHD-finger family of transcription factors. Plant J. **28,** 27–39.

Yang, S.L., Jiang, L., Puah, C.S., Xie, L.F., Zhang, X.Q., Chen, L.Q., Yang, W.C., and Ye, D. (2005). Overexpression of TAPETUM DETERMINANT 1 alters the cell fate in the Arabidopsis carpel and tapetum via genetic interaction with EXCESS MICROSPOROCYTES1/EXTRA SPOROGENOUS CELLS. Plant Physiol. **139,** 186–191.

Yang, S.Y., Xie, L.F., Mao, H.Z., Puah, C.P., Yang, W.C., Jiang, L., Sundaresan, V., and Ye, D. (2003). *TAPETUM DERTERMINANT1* is required for cell specialization in the Arabidopsis anther. Plant Cell **15,** 2792–2804.

Yang, W.C., Ye, D., Xu, J., and Sundaresan, V. (1999). The *SPOROCYTELESS* gene of Arabidopsis is required for initiation of sporogenesis and encodes a novel nuclear protein. Genes Dev. **13,** 2108–2117.

Zhao, D.Z., Wang, G.W., Speal, B., and Ma, H. (2002). The *EXCESS MICROSPOROCYTES1* gene encodes a putative leucine-rich repeat receptor protein kinase that controls somatic and reproductive cell fate in the Arabidopsis anther. Genes Dev. **16,** 2021–2031.

Zhou, A., Wang, H., Walker, J.-C., and Li, J. (2004). BRL1, a leucine-rich repeat receptor-like protein kinase, is functionally redundant with BRI1 in regulating *Arabidopsis* brassinosteroid signaling. Plant J. **40,** 399–409.